

## Dendrite growth in undercooled Al-rich Al-Ni melts measured on Earth and in Space

D. M. Herlach,<sup>1,2,3</sup> S. Burggraf,<sup>1,2</sup> M. Reinartz,<sup>3</sup> P. K. Galenko,<sup>3</sup> M. Rettenmayr,<sup>3</sup> Ch.-A. Gandin,<sup>4</sup> H. Henein,<sup>5</sup> A. Mullis,<sup>6</sup> A. Ilbagi,<sup>5</sup> and J. Valloton<sup>5</sup>

<sup>1</sup>*Institut für Materialphysik im Weltraum, Deutsches Zentrum für Luft- und Raumfahrt (DLR), 51170 Köln, Germany*

<sup>2</sup>*Institut für Experimentalphysik IV, Ruhr-Universität, 44780 Bochum, Germany*

<sup>3</sup>*Otto Schott Institut für Materialforschung, Friedrich-Schiller-Universität, 07743 Jena, Germany*

<sup>4</sup>*Centre de Mise en Forme des Matériaux, MINES ParisTech, 06904 Sophia Antipolis Cedex, France*

<sup>5</sup>*Advanced Materials and Processing Laboratory, University of Alberta, Edmonton AB T6G 1H9, Canada*

<sup>6</sup>*School of Chemical and Process Engineering, University of Leeds, Leeds LS2-9JT, United Kingdom*



(Received 4 February 2019; published 16 July 2019)

The dendrite growth velocity in  $\text{Al}_{75}\text{Ni}_{25}$  melts has been measured in a containerless procedure as a function of undercooling using an electromagnetic levitation technique both in the Earth laboratory and in Space on board the International Space Station. The growth shows an anomalous behavior inasmuch as the growth velocity decreases with increasing undercooling, confirming previous experiments on Earth. Within the scatter of experimental data, results obtained on Earth and in Space do not show significant differences. Thus, convection effects as the origin of the anomalous growth characteristics can be excluded. However, high-speed video recording exhibits multiple nucleation events in front of the growing solid-liquid interface. This effect is identified as the origin of the anomalous dendrite growth characteristics in undercooled melts of Al-rich Al-Ni melts.

DOI: [10.1103/PhysRevMaterials.3.073402](https://doi.org/10.1103/PhysRevMaterials.3.073402)

### I. INTRODUCTION

The properties of materials produced by solidification from melts are governed by crystal nucleation and subsequent crystal growth. Each solidification process needs an undercooling prior to solidification in order to initiate crystal nucleation and to drive the solidification front. At small undercoolings, a stable solid phase is formed whereas at large undercoolings the excess Gibbs free energy of the liquid also allows the solidification of metastable solid phases. Hence the profound understanding of these processes is of fundamental importance for materials design from the melt and materials processing [1,2]. Nucleation [3] and dendrite growth [2] have been intensely studied during the past. As far as dendrite growth is concerned, the velocity of the dendrites propagating through the volume of the melt has been measured as a function of undercooling [2]. By far in most cases, the velocity monotonically increases with increasing undercooling. Within the theory of dendrite growth this is easily understood by the fact that the driving force for growth is also continuously increasing with undercooling.

More recently, an opposite behavior has been found. One may distinguish two different cases. In glass-forming metallic alloys, the growth velocity  $V$  increases with undercooling  $\Delta T$ , but passes through a maximum and decreases with further increase of the undercooling. This has been verified in electrostatic levitation experiments of CuZr and NiZr, in which large undercoolings are achieved ranging up to the temperature regime above the glass transition temperature [4–6]. The observation of a maximum in  $V(\Delta T)$  has been explained by a competition of the counteracting effects of the driving force which increases with undercooling on the one hand, and the strong decrease of atomic diffusion with the increase

of undercooling on the other hand. At small undercoolings the driving force dominates, whereas at large undercoolings the decreasing atomic diffusion controls the growth kinetics. Alternatively, a negative gradient in the growth velocity versus undercooling relation has been reported for Al-rich Al-Ni alloys too [7]. However, these alloys do not form metallic glasses, since their glass transition temperature is low compared with that of glass formers. In particular, the temperature at maximum undercoolings, even by containerless processing, is far above the glass transition temperature, wherein the strong decrease in atomic diffusion characteristic of glass formation is not encountered. This anomalous behavior of the growth kinetics in undercooled melts of Al-rich Al-Ni alloys is thus not yet understood.

In the present work, several physical effects are discussed as the origin of the anomalous growth behavior in Al-Ni alloys reported in [7]. These include forced convection by external electromagnetic fields, inverse melting, and phase competition during solidification. Recent simulations have analyzed the influence of convection on crystal growth [8] which has also been investigated experimentally during parabolic flights under conditions of reduced gravity [9]. The influence of forced convection on the growth kinetics as found in an  $\text{Al}_{50}\text{Ni}_{50}$  alloy [10] is investigated by comparative measurements of dendrite growth as a function of undercooling of an  $\text{Al}_{75}\text{Ni}_{25}$  alloy using electromagnetic levitation both on Earth and in Space. In space the forces needed for compensation of disturbing accelerations are much smaller than the electromagnetic forces needed to compensate the gravitational accelerations on Earth by about three orders of magnitude. Consequently, forced convection in the case of experiments in Space is very much reduced. Moreover, we investigate the effect of different growth kinetics of various phases which may

compete during solidification. Inverse melting [11] of the alloy is investigated for deep undercoolings. Eventually, we analyze high-quality video images taken by a high-speed video camera in electromagnetic levitation experiments in Space. Thanks to the reduced convection, the video frames allow for a direct observation of different solidification phenomena when the quiescent melt is deeply undercooled prior to solidification. That makes it possible to determine the physical origin of the anomalous growth behavior of Al-rich Al-Ni alloys, i.e., the negative gradient in the  $V(\Delta T)$  relation at large undercoolings. The results will also be compared with microtomography observations of impulse atomized (IA) droplets (a type of drop tube) where the droplets experience very limited convection during rapid solidification.

## II. EXPERIMENT

Samples were prepared from the high-purity alloy constituents (6N in the case of Al and 5N in the case of Ni) by arc melting in a high-purity Ar atmosphere. The growth velocity as a function of undercooling in the Earth laboratory was measured by an electromagnetic levitation facility that is equipped with a high-speed camera in order to observe the propagation of the solid-liquid interface during solidification. Equivalent experiments were conducted on board the International Space Station (ISS) in the reduced gravity environment using the multiuser facility Electro-Magnetic Levitator (EML) developed by the European Space Agency (ESA) and the German Aerospace Center (DLR). The EML has been in operation since 2014. Details of the experimental facilities are described elsewhere [12]. The IA experiments were carried out using 4N Al and Ni. The composition of the alloy atomized was  $\text{Al}_{80}\text{Ni}_{20}$  with a similar solidification path expected to the  $\text{Al}_{75}\text{Ni}_{25}$  studied using the EML. Details of the IA experiments are found elsewhere [13].

## III. RESULTS AND DISCUSSION

According to the phase diagram of Al-Ni several peritectic reactions are expected for the  $\text{Al}_{75}\text{Ni}_{25}$  alloy. Figure 1 gives a section of the Al-Ni phase diagram on the Al-rich side onto which is superimposed the temperatures at which velocity-undercooling measurements have been made. From the phase diagram it is obvious that three phases are involved in the peritectic reactions of Al-rich Al-Ni alloys. These are the intermetallic phases AlNi (B2 phase),  $\text{Al}_3\text{Ni}_2$  and  $\text{Al}_3\text{Ni}$ .

Figure 2 shows results of measurements of the crystal growth velocity measured on Earth (triangles) and in space (circles). The data obtained on the ground are taken from previous experiments published in Ref. [7]. In contrast to the measurements on the intermetallic compound  $\text{Al}_{50}\text{Ni}_{50}$  [9] no difference is found between measurements in reduced gravity and under terrestrial conditions within the scatter of the data. Consequently, convection effects in the growth kinetics can be ruled out to be the origin of the anomalous growth behavior.

In 1987, Blatter and von Allmen [14] detected a very unusual phase transformation behavior of a  $\text{Ti}_{70}\text{Cr}_{30}$  thin film evaporated on a tungsten substrate. Laser quenching preserved the initial amorphous phase, annealing the film at 1073 K yielded a crystalline  $\beta$  phase, and surprisingly subsequent

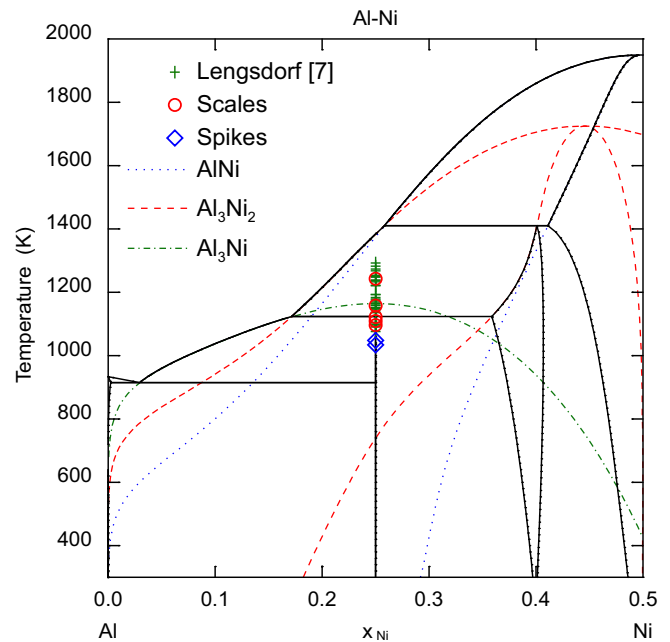


FIG. 1. Al-Ni phase diagram including metastable extensions of the liquidus and solidus lines for AlNi (dot),  $\text{Al}_3\text{Ni}_2$  (dash), and  $\text{AlNi}_3$  (dot-dash) phases. Also shown are the temperatures at which velocity measurements have been made for  $\text{Al}_{75}\text{Ni}_{25}$  on Earth by Lengsdorf *et al.* [7] and in microgravity.

annealing at 873 K restored the amorphous phase. If the amorphous phase is considered as a frozen liquid this finding was analyzed with respect to the phenomenon of inverse melting [9]. This means that during cooling of a liquid, the liquid transforms to a crystalline phase at a temperature  $T_x$  below the liquidus temperature  $T_L$ , but by further cooling the

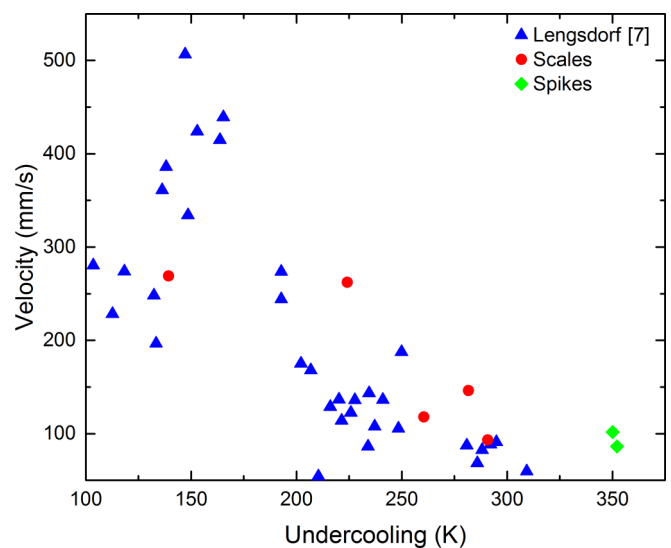


FIG. 2. Dendrite growth velocity as a function of undercooling measured on Earth (triangles) and in microgravity (circles) for alloy  $\text{Al}_{75}\text{Ni}_{25}$ . Data of the terrestrial experiments are taken from Ref. [7]. The color of the circles denotes the growth morphology observed by the high-speed camera, scales (red) and spikes (green).

liquid phase reappears at a temperature  $T_i < T_x < T_L$ ; i.e., the crystal remelts. This phenomenon would differ from the phase transformation behavior of binary alloys showing a retrograde monovariant line in their phase diagram. In this case, a crystal is formed at temperatures below the liquidus temperature and upon further cooling the crystal partly remelts. In this case remelting is associated with phase separation. On the other hand, inverse melting means complete remelting of the primary crystal upon cooling. Consequently, the Gibbs free energy of the liquid,  $G_l$ , and of the crystal,  $G_x$ , should cross twice if the temperature is continuously lowered from temperatures above the liquidus temperature  $T_l$ , first at a crystallization temperature  $T_x < T_l$ , and at the temperature of inverse melting  $T_i < T_x < T_l$ . It is remarkable that, from the viewpoint of thermodynamics, the liquid phase formed at  $T_i$  has to have a lower entropy  $S = -(\partial G/\partial T)_P$ . That is very unusual, certainly not possible in the case of pure metals. However, in the case of alloys the circumstances may differ. Neutron diffraction studies on deeply undercooled Al-Fe-Co [15,16] and  $\text{Ti}_{72.5}\text{Fe}_{27.5}$  [17] alloys show a rapid increase of the degree of both topological and chemical short-range order with increasing undercooling. On the other hand, solidification studies of deeply undercooled intermetallic phases give evidence of the formation of highly metastable disordered superlattice structures [18] which are characterized by a high entropy of the solid phase.

To further elucidate the hypothesis of inverse melting to be the origin of the anomalous growth kinetics of deeply undercooled Al-rich Al-Ni alloys we refer to *in situ* diffraction studies of phase selection in  $\text{Al}_{68.5}\text{Ni}_{31.5}$  [19] alloy using high-intensity synchrotron radiation. These experiments indicate primary crystallization of the B2 phase of intermetallic AlNi over the entire undercooling range accessible in the levitation experiments. After primary solidification, the metastable B2 phase transforms via a peritectic reaction to  $\text{Al}_3\text{Ni}_2$  at the corresponding peritectic temperature. In a third crystallization process, the intermetallic  $\text{Al}_3\text{Ni}$  phase is formed from  $L + \text{Al}_3\text{Ni}_2$ , where L stands for Liquid. The B2 phase does not form an amorphous phase as a Ti-Cr alloy. According to work by Turnbull, the glass transition temperature of such systems is expected to be very small, around  $0.3 T_l$  [20]. Taking  $T_l \approx 1950$  K for the AlNi B2 phase, its glass transition temperature is estimated to be around  $T_g \approx 585$  K. This means it is far away from the temperature of the undercooled melt, even at the maximum undercooling of  $\Delta T \approx 350$  K achieved in the space experiments;  $T \approx T_l - 350 \text{ K} \approx 1600$  K. Therefore, we exclude inverse melting to be the physical origin of the anomalous dendrite growth behavior of Al-rich Al-Ni alloys.

The investigations of phase selection during solidification of the undercooled melt of the  $\text{Al}_{75}\text{Ni}_{25}$  alloy indicate that three intermetallic phases, metastable AlNi,  $\text{Al}_3\text{Ni}_2$ , and  $\text{Al}_3\text{Ni}$ , are involved in the solidification process until the entire liquid is transformed to solid [21]. That is compatible with the temperature-time profiles recorded on  $\text{Al}_{75}\text{Ni}_{25}$  alloy during the space experiments. Figure 3 shows such a temperature-time profile recorded during solidification of an  $\text{Al}_{75}\text{Ni}_{25}$  sample upon an undercooling of  $\Delta T = 350$  K prior to solidification. Three reactions are visible through the release of the heat of transformations and its impact on the temperature curve measured. The first one is identified

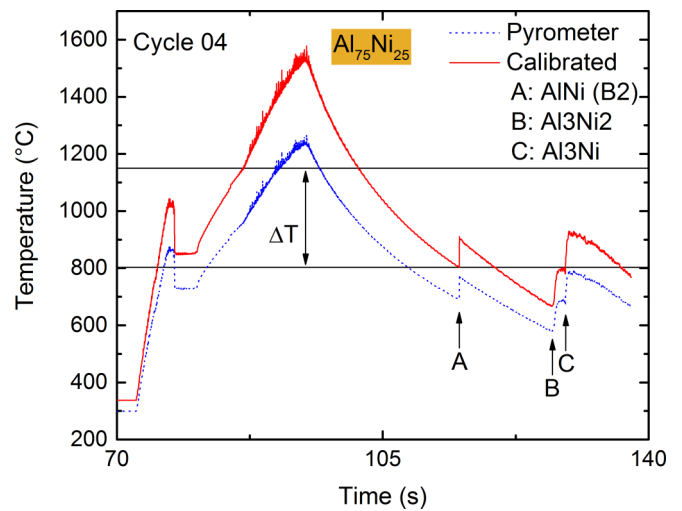


FIG. 3. Temperature-time profile measured during solidification of  $\text{Al}_{75}\text{Ni}_{25}$  in Space upon an undercooling of  $\Delta T \approx 350$  K. The red curve gives the data of the pyrometer calibrated by the correct emissivity. Three phase formation temperatures are observed labeled A–C.

as the primary crystallization of metastable AlNi B2 phase, the second one the peritectic reaction involving the  $\text{Al}_3\text{Ni}_2$  intermetallic phase, and the third one the formation of  $\text{Al}_3\text{Ni}$  phase from the  $L + \text{Al}_3\text{Ni}_2$  reaction. Further cooling could even have shown evidence of a fourth reaction due to the final eutectic transformation at lower temperature corresponding to the coupled growth of  $\text{Al}_3\text{Ni}$  and Al-rich lamellae [22]. It is emphasized that the distance on the time axis between the various phase reactions depends strongly on the undercooling achieved prior to solidification. Hence, it may be argued that a competition of various phases during solidification could lead to a negative gradient in the  $V(\Delta T)$  relationship provided the velocity measurements are integral and the volume phase fractions  $F$  depend essentially on the undercooling. Under such circumstances an average velocity  $V$  can be estimated as

$$V = \frac{(F_A V_A + F_B V_B + F_C V_C)}{F_A + F_B + F_C} \quad (1)$$

with A : AlNi; B :  $\text{Al}_3\text{Ni}_2$ ; C :  $\text{Al}_3\text{Ni}$ .

We have computed the dendrite growth velocities of the various phases involved in the solidification of  $\text{Al}_{75}\text{Ni}_{25}$  alloy using the sharp interface theory of dendrite growth in undercooled melts [23]. The results of these computations are shown in Fig. 4. All three curves show qualitatively the same characteristics: a monotonic increase with undercooling. Since the slope of all curves is very similar, it is very unlikely that the anomalous growth kinetics of  $\text{Al}_{75}\text{Ni}_{25}$  alloy can be understood according to Eq. (1) assuming a dependence of the phase fractions of the various phases with a change of undercooling.

Phase-field modeling has also been employed to simulate the growth of the B2 AlNi and  $\text{Ni}_2\text{Al}_3$  phases from their undercooled parent melt. This is a coupled thermosolutal simulation [24]; however, as a computational expedient the Lewis number,  $Le$  (= thermal diffusivity or solute diffusivity),

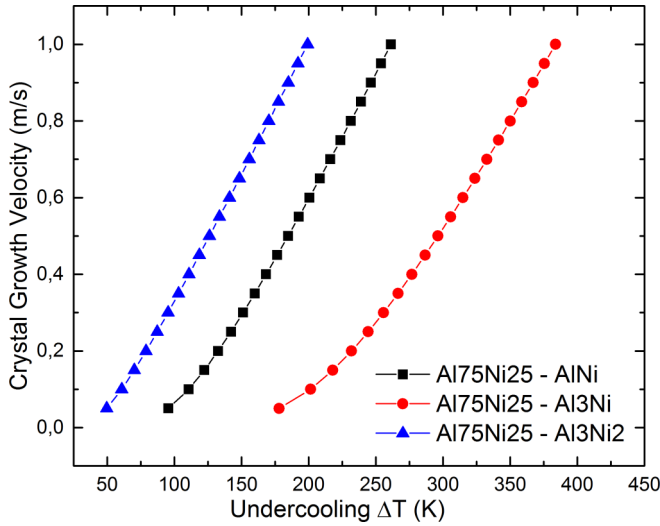


FIG. 4. Dendrite growth velocities as a function of undercooling of the various phases involved in the solidification of undercooled Al<sub>75</sub>Ni<sub>25</sub> alloy, AlNi (black), Al<sub>3</sub>Ni<sub>2</sub> (blue), and Al<sub>3</sub>Ni (red).

has been set artificially low to 100. Similar results are found as in the case of sharp interface modeling (cf. Fig. 4), as demonstrated in Fig. 5. The most obvious discrepancy is that, as with all standard materials, the growth velocity increases with increasing undercooling, rather than decreasing as observed experimentally. This poor agreement between observation and model, which is not only quantitative but also qualitative (i.e., the incorrect trend is observed) would suggest that either (i) there is some unique physics for the Al-Ni system which is not considered in the existing model, or (ii) the behavior of the Al-Ni system could in principle be described by the physics already built into the model but, for whatever reason, this behavior is not captured with sufficient fidelity. The response of the system to increasing Lewis number may be instructive. Increasing Le from 100 to 500 resulted in an average increase

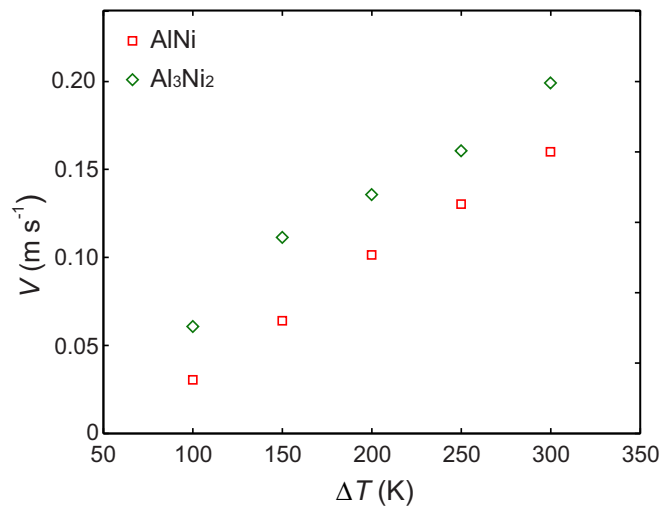


FIG. 5. Calculated growth velocity as a function of undercooling estimated from the coupled thermosolutal phase-field model. Calculation shown for primary growth of both AlNi and of Al<sub>3</sub>Ni<sub>2</sub> in an undercooled melt of the Al<sub>70</sub>Ni<sub>30</sub> alloy.

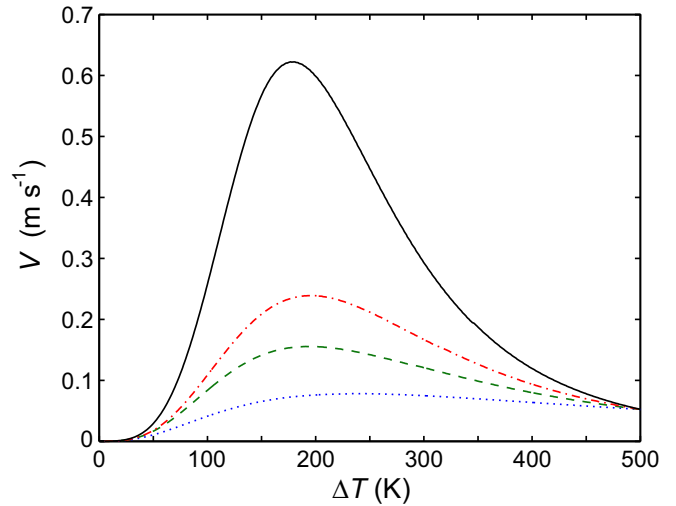


FIG. 6. Exemplary LKT type calculations using undercooling dependent  $|m|$  and  $k_E$ . ( $|m|$  increasing with  $\Delta T$  and  $k_E$  decreasing with  $\Delta T$ ): Dots: both  $|m|$  and  $k_E$  linear; dash:  $|m|$  convex down and  $k_E$  linear; dot-dash:  $|m|$  linear and  $k_E$  convex up; solid:  $|m|$  convex down and  $k_E$  convex up.

in  $V$  of 27%, while further increases in Le had minimal effect on  $V$ . This is in contrast to previous investigations on solid solution alloys [25], where a similar increase in Le resulted in an increase of 290% in the growth velocity  $V$ , while increasing further from Le = 500 to Le = 10 000 leads to a further 400% increase in  $V$ . This would suggest growth in Al-Ni is under full solutal control, which would be consistent with the very steep slope of the liquidus line,  $|m| = 41.74 \text{ K at. \%}^{-1}$  and  $|m| = 32.27 \text{ K at. \%}^{-1}$  for AlNi and Al<sub>3</sub>Ni<sub>2</sub>, respectively, at 1300 K and  $c = 30 \text{ at. \% Ni}$ . Consequently, very small changes in the solute concentration at the tip could potentially lead to large variations in the interface temperature.

This is significant, as preliminary investigations using the Lipton Kurz Trivedi (LKT) model [26] for dendritic solidification, including a description of solidus and liquidus lines that are functions of  $T$ , indicate that the type of inverse velocity trend observed in Al-Ni could potentially be explained without recourse to any novel physics. In Fig. 6 we show the LKT curves in which  $|m|$  and  $k_E$  are a function of  $\Delta T$  (i.e., also of  $T$ ).  $|m|$  increasing with  $\Delta T$  and  $k_E$  decreasing with  $\Delta T$  will both favor lower growth velocity and, with sufficiently rapid change, can overcome the natural tendency for the velocity to increase with increasing  $\Delta T$ . However, the form of the dependence of  $|m|$  and  $k_E$  upon  $\Delta T$  is also important. A more marked inverse velocity trend is favored if  $|m|$  plotted against  $\Delta T$  is convex downwards and  $k_E$  plotted against  $\Delta T$  is convex upwards. This is illustrated in Fig. 6 which shows the effect of a linear variation of  $|m|$  and  $k_E$  (blue),  $|m|$  only convex (red),  $k_E$  only convex (magenta), and both convex (green). All the curves display some common characteristics, including an initially increasing velocity followed by a local maximum beyond which the velocity decreases with further increases in  $\Delta T$ . This type of behavior is exactly as displayed by the Al<sub>75</sub>Ni<sub>25</sub> alloy (cf. Fig. 2). It is not explicitly displayed by the other Al-Ni alloys, but according to the (plausible) assumption that  $V = 0$  at  $\Delta T = 0$ , a local maximum must be present for

all the other alloys, but at lower undercooling than assessed in the experiments reported [7]. However, the values taken for  $|m|$  and  $k_E$  to produce the maximum in the computed growth velocity as a function of undercooling are not compatible with the phase diagram of Al-rich Al-Ni alloys.

It is noted that the diffusion coefficient is assumed to be nearly constant. This is justified by the fact that the undercooling temperatures are far away from the region near the glass transition temperatures where the diffusion coefficient rapidly decreases with decreasing temperature. Indeed, in glass-forming systems like CuZr [4] and NiZr [5] the rapidly decreasing diffusion coefficient counteracts the rapidly increasing driving force (Gibbs free energy) when the undercooling temperatures approach the temperature range above the glass temperature. In the Zr-based glass-forming alloys electrostatic levitation is capable of producing undercoolings which enter the region near the glass transition temperature  $T_g$  since the relative glass temperatures  $T_g/T_L$  ( $T_L$ : liquidus temperature) are much higher than in Al-Ni alloys. This causes a maximum in the velocity-undercooling relation in glass-forming systems but this effect is not relevant in explaining the negative temperature gradient in the velocity-undercooling relation of Al-Ni alloys.

From the discussion so far it is concluded that the anomalous growth kinetics will not be directly related to the crystal growth mechanism. This assumption is supported by plotting the velocity not as a function of undercooling, but as a function of the nucleation temperature  $T_N$ . The majority of the data points for  $x \leq 35$  at. % Ni follow a single trend, as shown in Fig. 7. This behavior is unusual. A common trend of velocity against  $T_N$  across alloys of different composition would not be expected; the variation in liquidus temperature with alloy composition means that a fixed value of  $T_N$  can map onto widely differing values of  $\Delta T$  for the different alloys.

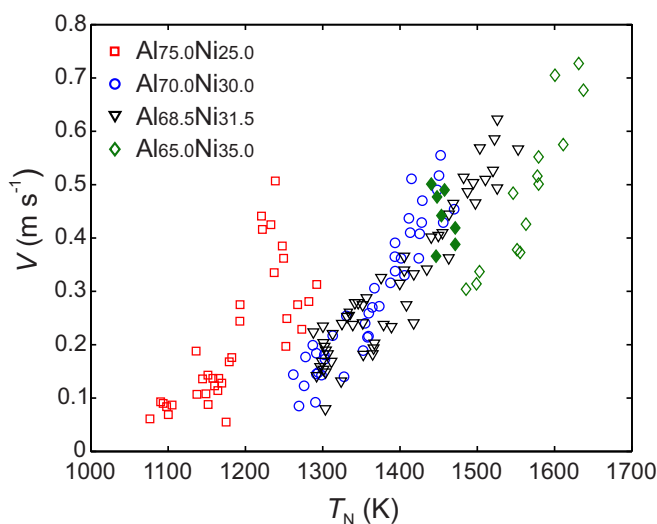


FIG. 7. Growth velocity for Al- $x$  at. % Ni ( $x = 25, 30, 31.5,$  and  $35$ ) as a function of nucleation temperature,  $T_N$ . Open symbols = inverse velocity trend ( $V$  decreasing with  $\Delta T$ ); filled symbols = normal velocity trend ( $V$  increasing with  $\Delta T$ ). Most data follow a single trend with  $T_N$ .

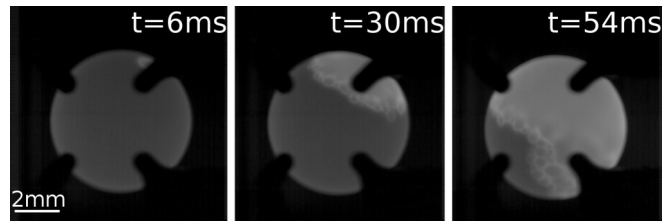


FIG. 8. Image sequence of the high-speed camera of an  $\text{Al}_{75}\text{Ni}_{25}$  alloy solidified in microgravity at an undercooling of  $\Delta T = 282$  K using the ISS-EML multiuser facility.

The specific conditions of reduced gravity with a quiescent state of the freely suspended liquid drop give favorable conditions for the direct observation of the intersection line of the sample surface and the dendritic solidification front, and the processes running in this region during propagation of the solid-liquid interface through the sample. Figure 8 shows an image sequence from the high-speed camera taken during solidification of the  $\text{Al}_{75}\text{Ni}_{25}$  alloy upon undercooling of  $\Delta T = 282$  K in Space. The video illustrates that the growth front is built by sequential nucleation events propagating along the surface; we denote them as *scales*.

The observed growth front is a front of multiple nucleation events propagating along the sample surface. In Fig. 9 the crystals are bounded by circles. Multiple nucleation events have also been observed in submillimeter  $\text{Al}_{80}\text{Ni}_{20}$  droplets solidified using the impulse atomization technique, a drop-tube type technique [13]. Rapid solidification of the samples occurs during free fall with reduced convection. Figure 10 shows selected synchrotron x-ray microtomography slices of a  $310\text{-}\mu\text{m}$ -diameter droplet atomized in helium. Several

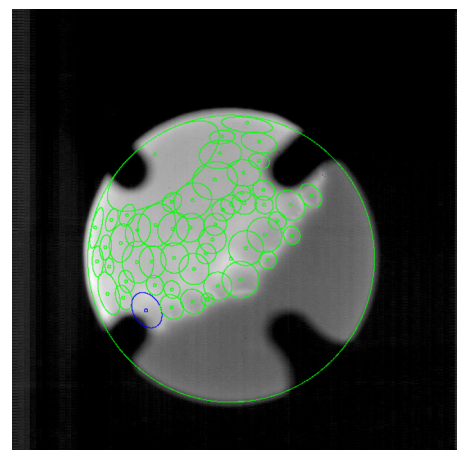


FIG. 9. Image taken from the high-speed camera video during solidification of a  $\text{Al}_{75}\text{Ni}_{25}$  sample upon an undercooling of  $291$  K prior to solidification using the EML on board the ISS. The green circles adumbrate the crystals which are formed by copious nucleation in front of the propagating solid-liquid interface. The first nucleation event was on the upper left side (large circle). Evaluation of experiments performed on board the International Space Station in June 2017.

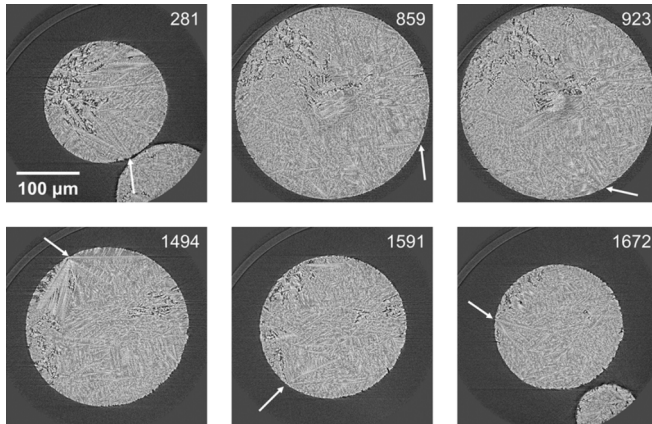


FIG. 10. Selected synchrotron x-ray microtomography slices of a 310- $\mu\text{m}$   $\text{Al}_{80}\text{Ni}_{20}$  droplet atomized in helium. The arrows denote nucleation points at the surface of the droplets with primary dendrite arms growing towards the center of the droplet.

nucleation points are observed at the surface of the droplet. Similarly to EML samples, dendrites grow towards the center of the droplet.

A feedback mechanism is put forward to explain the decreasing velocity with increasing undercooling. The increase in temperature and change in composition influence the active layer of nucleation around the growing dendrite. Crystal nucleation and growth lead to the release of heat and rejection of solute from the solid-liquid interface, which is expected to impede nucleation in the vicinity of already existing nuclei.

In the temperature range far away from the glass temperature, as in the present case of Al-Ni alloy, the nucle-

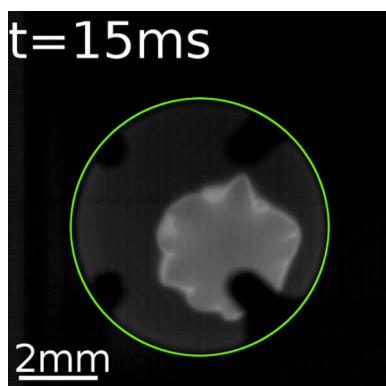


FIG. 11. A spiked morphology is observed during solidification of an  $\text{Al}_{75}\text{Ni}_{25}$  alloy undercooled by  $\Delta T = 350$  K in the microgravity environment. Such a morphology has not yet been observed on Earth. The green circle marks the sample outline. It is emphasized that the microgravity experiments give the benefit of a strong reduction of convective flow. This special experimental condition made it possible to observe not only the spiked morphology but also the copious crystallization in front of the solid-liquid interface that may be the origin of the anomalous growth behavior of undercooled Al-rich Al-Ni alloys.

ation rate rapidly increases with undercooling. That means that the amount of heat released at the solidification front by copious crystallization is large enough to prevent further undercooling to proceed. As a consequence, the reduction of the growth velocity continuously increases with increasing undercooling. The higher the undercooling the higher the nucleation rate and, hence, the heat released in front of the solid-liquid interface. As a consequence, the driving force for the advancement of the solidification front becomes reduced with further increasing the undercooling with the consequence of reduction of growth velocity.

A *scales* morphology has been observed at undercoolings  $\Delta T < 300$  K (cf. also the red circles in Fig. 2). At larger undercoolings of  $\Delta T > 300$  K, the morphology of the solidification front changes. Figure 11 shows an image taken from the high-speed camera recorded during solidification of an  $\text{Al}_{75}\text{Ni}_{25}$  sample undercooled by  $\Delta T = 350$  K prior to solidification. The morphology of the solidification front differs from Figs. 8 and 9 in that *spikes* on a macroscopic scale are formed which are not visible during solidification of the same sample at smaller undercoolings. We denote such structures as spiked morphology (cf. green circles in Fig. 2). This has not been observed in terrestrial experiments. This morphology does not show the circular shape of the nuclei but an anisotropic shape.

#### IV. CONCLUSIONS

The solidification behavior of undercooled melts of Al-rich Al-Ni alloys has been investigated and discussed. In particular, the anomalous growth dynamics; i.e., the decrease of the growth velocity with increasing driving force for crystallization (undercooling) was analyzed with respect to various physical phenomena. Possible effects of forced convective flow inside the liquid sample have been studied by comparing experimental measurements of the dendrite growth velocity as a function of undercooling of  $\text{Al}_{75}\text{Ni}_{25}$  samples using electromagnetic levitation on Earth (strong fluid flow) and microgravity on board the International Space Station. Also, inverse melting was the subject of the search of the physical origin of anomalous dendrite growth. Dendrite growth in undercooled melts of Al-rich Al-Ni samples was simulated both by phase field and sharp interface modeling, in particular proving the growth kinetics of the intermetallic phases of metastable  $\text{AlNi}$ ,  $\text{Al}_3\text{Ni}_2$ , and  $\text{Al}_3\text{Ni}$  which are involved in the complete solidification process of the Al-rich Al-Ni alloys. None of these investigations led to a convincing explanation of the anomalous growth characteristics of the alloys investigated. However, the space experiments allowed very clear recording of temperature-time profiles and high-speed camera videos of the propagating solidification front during solidification of the undercooled melt. That was possible since the levitated liquid drops behave much more quiescently in Space compared with levitation on Earth. The reason is that levitation on Earth needs much higher levitation forces to compensate the gravitational force than the positioning forces in reduced gravity to compensate disturbing accelerations. Thus, the external influence of the alternating electromagnetic fields both on the oscillations of the drop inside the coil

systems as well as the internal fluid flow motion inside the drop is very much reduced in Space. The results of these measurements allowed us to directly detect and observe multiple nucleation events in front of the solid-liquid interface. Since copious nucleation leads to the release of the heat of crystallization, it leads to a reduction of the temperature gradient in front of the interface and hence to a reduction of the dendrite growth velocity. The nucleation rate steeply rising with increasing undercooling, the effect of copious nucleation becomes stronger with increasing undercooling and leads to a monotonous decrease of the dendrite growth velocity with increasing undercooling.

## ACKNOWLEDGMENTS

The authors acknowledge access to the ISS-EML, which is a joint undertaking of the European Space Agency (ESA) and the DLR Space Administration. The reported work was conducted in the framework of the ESA research project NEQUISOL (15236/02//NL/SH). The authors thank Dr. Wim Sillekens as the representative of ESA for always constructive cooperation. The authors thank A. L. Greer for focusing our interest on inverse melting as a possible reason for anomalous dendrite growth in Al-Ni alloy melts. We thank HYDRO Aluminium Deutschland for delivering the high-purity Al for simple preparation.

- 
- [1] M. Asta, C. Beckermann, A. Karma, W. Kurz, R. Napolitano, M. Plapp, G. Purdy, M. Rappaz, and R. Trivedi, Solidification microstructures and solid-state parallels: Recent developments, future directions, *Acta Mater.* **57**, 941 (2009).
- [2] D. M. Herlach, P. Galenko, and D. Holland-Moritz, in *Metastable Solids from Undercooled Melts*, edited by R. W. Cahn, Pergamon Materials Series (Elsevier, Oxford, 2007).
- [3] K. F. Kelton and A. L. Greer, *Nucleation in Condensed Matter: Applications in Materials and Biology* (Elsevier, Amsterdam, 2010).
- [4] H. Wang, D. M. Herlach, and R. Liu, Dendrite growth in  $\text{Cu}_{50}\text{Zr}_{50}$  glass-forming melts, thermodynamics versus kinetics, *EPL* **105**, 36001 (2014).
- [5] R. Kobold, W. W. Kuang, H. Wang, W. Hornfeck, M. Kolbe, and D. M. Herlach, Dendrite growth velocity in the undercooled melt of glass forming  $\text{Ni}_{50}\text{Zr}_{50}$  compound, *Philos. Mag. Lett.* **97**, 249 (2017).
- [6] D. M. Herlach, S. Burggraf, P. K. Galenko, C.-A. Gandin, A. Garcia-Escorial, H. Henein, C. Karrasch, A. Mulis, M. Rettenmayr, and J. Valloton, Solidification of undercooled melts of Al-based alloys on Earth and in Space, *JOM* **69**, 1303 (2017).
- [7] R. Lengsdorf, D. Holland-Moritz, and D. M. Herlach, Anomalous dendrite growth in undercooled melts of Al-Ni alloys in relation to results obtained in reduced gravity, *Scr. Mater.* **62**, 365 (2010).
- [8] H. Peng, D. M. Herlach, and T. Voigtmann, Crystal growth in fluid flow: Nonlinear response effects, *Phys. Rev. Mater.* **1**, 030401(R) (2017).
- [9] S. Binder, M. Kolbe, S. Klein, and D. M. Herlach, Solidification of tetragonal  $\text{Ni}_2\text{B}$  from the undercooled melt, *EPL* **97**, 36003 (2012).
- [10] S. Reutzel, H. Hartmann, P. K. Galenko, S. Schneider, and D. M. Herlach, Change of the kinetics of solidification and microstructure formation induced by convection in the Ni-Al system, *Appl. Phys. Lett.* **91**, 041913 (2007).
- [11] A. L. Greer, The thermodynamics of inverse melting, *J. Less-Common Met.* **140**, 327 (1988).
- [12] D. M. Herlach, Non-equilibrium solidification of undercooled melts, *Metals* **4**, 196 (2014).
- [13] A. Ilbagi, P. Delshad Khatibi, I. P. Swainson, G. Reinhart, and H. Henein, Microstructural analysis of rapidly solidified aluminium-nickel alloys, *Can. Metall. Q.* **50**, 295 (2011).
- [14] A. Blatter and M. von Allmen, Reversible Amorphization in Laser-Quenched Titanium Alloys, *Phys. Rev. Lett.* **54**, 2103 (1985).
- [15] T. Schenk, V. Simonet, D. Holland-Moritz, R. Bellissent, T. Hansen, P. Convert, and D. M. Herlach, Temperature dependence of the chemical and topological short-range order in undercooled and stable Al-Fe-Co liquids, *EPL* **65**, 34 (2004).
- [16] D. Holland-Moritz, T. Schenk, V. Simonet, R. Bellissent, P. Convert, T. Hansen, and D. M. Herlach, Short range order in undercooled metallic liquids, *Mater. Sci. Eng., A* **375-377**, 98 (2004).
- [17] D. Holland-Moritz, O. Heinen, R. Bellissent, T. Schenk, and D. M. Herlach, Short-range order of liquid  $\text{Ti}_{72.3}\text{Fe}_{27.7}$  investigated by a combination of neutron scattering and x-ray diffraction, *Int. J. Mater. Res.* **97**, 948 (2006).
- [18] H. Hartmann, D. Holland-Moritz, P. Galenko, and D. M. Herlach, Evidence of the transition from ordered to disordered growth during rapid solidification of an intermetallic phase, *Europhys. Lett.* **87**, 40007 (2009).
- [19] O. Shuleshova, D. Holland-Moritz, W. Löser, G. Reinhart, G. N. Iles, and B. Büchner, Metastable formation of decagonal quasicrystals during solidification of undercooled Al-Ni melts: In situ observations by synchrotron radiation, *EPL* **86**, 36002 (2009).
- [20] D. Turnbull, Under what conditions can a glass be formed? *Contemp. Phys.* **10**, 473 (1969).
- [21] D. Tourret, G. Reinhart, Ch.-A. Gandin, G. N. Iles, U. Dahlborg, M. Calvo-Dahlborg, and C. M. Bao, Gas atomization of Al-Ni powders: Solidification modelling and neutron diffraction analysis, *Acta Mater.* **59**, 6658 (2011).
- [22] D. Tourret, Ch.-A. Gandin, T. Volkman, and D. M. Herlach, Multiple non-equilibrium phase transformations: Modeling versus electro-magnetic levitation experiment, *Acta Mater.* **59**, 4665 (2011).
- [23] P. K. Galenko and D. A. Danilov, Model for free dendritic alloy growth under interfacial and bulk phase nonequilibrium conditions, *J. Cryst. Growth* **197**, 992 (1999).
- [24] P. C. Bollada, C. E. Goodyer, P. K. Jimack, A. M. Mullis, and F. W. Yang, Three dimensional thermal-solute phase field simulation of binary alloy solidification, *J. Comput. Phys.* **287**, 130 (2015).
- [25] J. Rosam, P. K. Jimack, and A. M. Mullis, Quantitative phase-field modeling of solidification at high Lewis number, *Phys. Rev. E* **79**, 030601(R) (2009).
- [26] J. Lipton, W. Kurz, and R. Trivedi, Rapid dendrite growth in undercooled alloys, *Acta Metall.* **35**, 957 (1987).